Scientific paper

Practical Design Criteria for Saturated Pseudo Strain Hardening Behavior in ECC

Tetsushi Kanda[1] and Victor C. Li[2]

Received 14 October 2005, accepted 5 December 2005

Abstract

Engineered Cementitious Composites (ECCs) have recently demonstrated their high performance with pseudo strain hardening (PSH) behavior in civil engineering structures and buildings. These materials incorporate low cost fibers such as Polyvinyl Alcohol fibers, which often rupture in composites. Such fiber rupture type ECCs tend to have inferior and unsaturated PSH behavior compared with those incorporating properly designed pull out type fiber. The present study focuses on presenting practical design criteria to achieve saturated PSH behavior in fiber rupture type ECCs. These criteria are proposed based on two performance indices, which are measures of energy exchange during steady state flat crack propagation and stress level to initiate micro-cracks. The latter performance index necessitates a new cracking strength prediction theory, which is proposed in the current study. Finally the cracking strength theory is justified using tensile test data, and the criteria are proposed based on the data in terms of these two indices.

1. Introduction

Fiber reinforced cement composites with pseudo strain hardening (PSH, hereafter) behavior have been extensively investigated in the world and are expected to provide impact on realizing innovative infrastructure (Naaman and Reinhardt 1995). Engineered Cementitious Composite (ECC) (Li 1993), a special version of PSH cementitious composites, has already been applied in several structures and demonstrated its high performance on site. These applied ECCs involved relatively low cost fiber such as a Polyvinyl Alcohol (PVA) fiber. This kind of composites often involves fiber rupture in crack bridging action due to the combination of relatively moderate fiber strength, small fiber diameter and strong chemical bonding. This composite type is therefore named fiber rupture type ECC in the current study. A Micromechanics based composite design theory has been proposed (Kanda and Li 1999), which enables one to design the fiber rupture type ECCs, based on micromechanics constitutive properties including chemical bond strength in fiber/matrix interface and fiber's in-situ strength in composites.

The fiber rupture type ECCs with PVA fibers (Kanda and Li 1999) tend to have lower strain capacity than composites with no fiber rupture (fiber pull-out type composites) such as those reinforced with 40μm diameter Polyethylene fiber (Li *et al*. 1995). This 40μm-Polyethylene fiber composite showed over 5 % strain capacity, and its PSH behavior is classified as "saturated PSH behavior", in contrast to "unsaturated PSH behavior" of the PVA fiber composites. The extent of PSH is associated with saturation intensity of multiple cracking sequence and has been investigated both experimentally and theoretically (Kanda and Li 1998; Kanda and Li 1999). These investigations revealed that the PVA fiber composites have lower available complementary energy in crack bridging than the Polyethylene fiber composites. This lower energy performance appears responsible for the inferior strain capacity or unsaturated PSH behavior of the PVA fiber composites. While recent research progress has demonstrated substantially improved strain performance in PVA-ECC by adopting interface tailoring (Li *et al*. 2002), the criteria for achieving saturated PSH in the fiber rupture type ECCs need further clarification.

It has been demonstrated that stress performance is also important for the saturated PSH behavior as well as energy performance. It was proposed that these two performances are measured by two indices, stress performance index and energy performance index (Kanda and Li 1998). These two indices were shown to reasonably represent composite potential for PSH behavior. In addition, two practical design criteria using these indices were presented for saturated PSH in fiber pull-out type composites. These performance indices and practical design criteria should be extended to cover fiber rupture type composites. This extension requires better understanding of the tensile behavior of the fiber rupture type composites. The stress performance index involves first cracking strength, which has not been theoretically clarified in literature for the fiber rupture type ECC but has been for fiber pull-out type (Li and Leung 1992).

The present study focuses on presenting the practical criteria to facilitate designing saturated PSH behavior in fiber rupture type ECC. To achieve this goal, two per-

[1]Supervisory Research Engineer, Kajima Technical Research Institute, Japan.
E-mail: kandat@kajima.com
[2]Professor, Department of Civil and Environmental Engineering, Department of Materials Science and Engineering, University of Michigan, USA.

formance indices and corresponding design criteria are proposed by extension of previous research results for fiber pull-out type composites. The first cracking strength can be determined using micromechanics concepts of bridged cracks. For this determination, a new first cracking strength estimation scheme is proposed involving fiber rupture. Next, composites involving fiber rupture are designed potentially to show variety of PSH saturation and are then tested under uniaxial tensile loading. Findings in this test combined with preliminary published work are used in the current study to justify the cracking strength theory and to establish the criteria for achieving saturated PSH behavior.

2. Performance indices

Two performance indices were proposed to describe tensile strain performance of the fiber pull-out type ECCs (Kanda and Li 1998). These two indices were obtained from the primary conditions for PSH behavior as follows (Leung 1996; Li 1993; Li and Leung 1992).

$$(\sigma_{fc})_i < \sigma_{peak} \tag{1}$$

$$J_{tip} < J'_b \tag{2}$$

where, $(\sigma_{fc})_i$ is the first cracking strength, σ_{peak} is the peak of crack bridging stress σ_c due to fiber in composite, J_{tip} is the crack tip toughness of composite, and J'_b is complementary energy (Marshall and Cox 1988) of the σ_c-δ curve. δ denotes crack opening displacement (COD). In principle, all four parameters can vary from one (potential) crack plane to another. However, this study focuses on the variability of $(\sigma_{fc})_i$. The implication of eq. (1) can be intuitively understood, namely, that the crack bridging stress of a composite should be higher than the first cracking strength, otherwise the composite fails immediately after a microcrack is initiated from a defect site. eq. (2) implies that sufficient energy should be supplied to create steady state crack condition necessary for multiple crack generation. This implication is explained by **Fig. 1**, which illustrates the σ_c-δ curve. The area under this curve shows the energy consumed by fiber bridging action per unit crack advance. This bridging energy is well know as a source of better ductility of conventional fiber reinforced concrete (e.g., Hirsch 1962; e.g., Ogishi and Ono 1987). On the other hand, the complementary energy J'_b is understood as the net energy available for crack propagation (difference between externally supplied work and fiber bridging energy consumption), while J_{tip} represents the matrix crack toughness resisting the propagation. Hence eq. (2) expresses that the maximum energy available for steady state crack propagation should exceed energy necessary to break down the matrix. A more detailed explanation for eq. (2) can be found in Marshall and Cox (1988) and Li (1993).

Performance indices $\sigma_{peak}/(\sigma_{fc})_i$ (stress performance index) and J'_b/J_{tip}, (energy performance index) are proposed in according with eq. (1) and eq. (2). Both these performance indices must exceed unity for realizing PSH behavior for the fiber pull-out type ECC (Kanda and Li 1998). The assumption behind this concept is that σ_{peak} and J'_b may not reach their expected theoretical values in a given material/specimen due to matrix and fiber bridging variability. $\sigma_{peak}/(\sigma_{fc})_i$ and J'_b/J_{tip}, therefore represent "margins" of strength and energy performance. Higher index values imply greater possibility of saturated multiple cracking or saturated PSH behavior, which result in higher strain capacity. Estimating the performance indices requires knowledge of the σ_c-δ relation. This representation has been demonstrated in a previous study (Kanda and Li 1999). σ_c in normalized form was expressed as a function of micromechanics parameters of composite constituents in addition to δ,

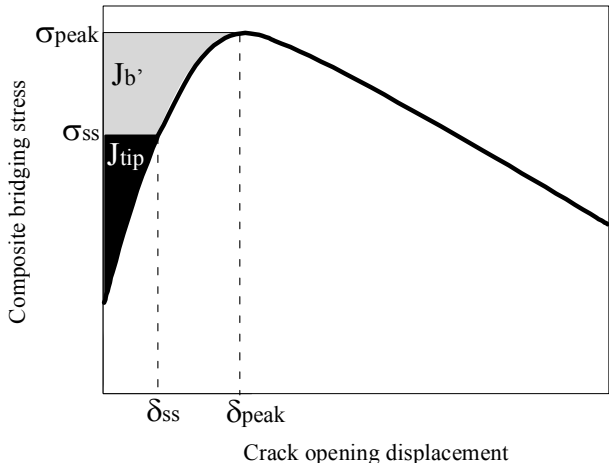

Fig. 1 Energy condition for Pseudo Strain Hardening.

$$\bar{\sigma}_c = func.\left(\bar{\delta}; \frac{E_f}{\lambda}, \frac{\sigma_{ds}}{\lambda}, \frac{\sigma_{fu}^n}{\lambda}, f, f',\right) \tag{3}$$

where,

$$\bar{\sigma}_c = \frac{\sigma_c}{V_f E_f / 4},\ \bar{\delta} = (1+\eta)\hat{\delta},\ \hat{\delta} = \frac{2\delta}{L_f},\ \eta = \frac{V_f E_f}{(1-V_f)E_m}$$

V_f = volume fraction of fiber

E_f = elastic modulus of fiber

E_m = elastic modulus of matrix

$$\lambda \equiv 2\tau_i \left(L_f / d_f\right),\ \sigma_{ds} \equiv 2(1+\eta)\left(\frac{\tau_s}{\rho}\right)$$

τ_i = interfacial frictiona bond strength

L_f = fiber length

d_f = fiber diameter

$$\rho^2 = 2G_c E_c \Big/ \left[\left(1-V_f\right) E_m E_f \log\left(\frac{2R^*}{d_f}\right) \right]$$

τ_s = Chemical bond strength

E_c = Elastic modulus of composite

G_c = Shear modulus of composite

R^* = Effective radius of matrix cylinder containing the fiber

f = Snubbing coefficient

f' = Fiber strength reduction factor

Snubbing coefficient f was introduced to express enhancing effects of fiber inclining angle on single fiber's pulled out resistance load. More details are to be referred to a literature (Li *et al*. 1990). The full expression of eq. (3), or bridging law, is shown in Appendix. Then the complementary energy J'_b is given by (Marshall and Cox 1988):

$$J_{tip} \leq J'_b = \sigma_{peak}\delta_{peak} - \int_0^{\delta_{peak}} \sigma_c(\delta)d\delta \qquad (4)$$

where,

σ_{peak} =Peak stress of $\sigma_c(\delta)$

$\delta_{peak} = \delta$ corresponding to σ_{peak}

Equation (4) was numerically evaluated using the bridging law of eq. (3) (Kanda and Li 1999). In this reference, the calculated J'_b/J_{tip} was substantiated via a limited number of examples to be useful in predicting the behavior of fiber rupture type composites. The current study adopts the same procedure for calculating J'_b/J_{tip} but applied it to a broader range of composites.

The other performance index requires the evaluation of $\sigma_{peak}/(\sigma_{fc})_i$ and therefore the theoretical examination of $(\sigma_{fc})_i$. This is discussed next.

3. Theory for first cracking strength

A fundamental approach for deriving $(\sigma_{fc})_i$ suggested in past researches (Li and Leung 1992; Marshall and Cox 1988) was based on fracture mechanics. In these literatures, a simple penny shape flaw involved in composite body, which is bridged by short random fibers as illustrated in **Fig. 2**. Following the notation by Li and Leung, the net stress intensity factors must balance the crack tip fracture toughness when composite cracking occurs:

$$\hat{K}_L + \hat{K}_B = \hat{K}_{tip} \qquad (5)$$

where,

$$\hat{K}_L = K_L \Big/ \left(\sigma_{0i}\sqrt{c_0}\right)$$

$$\hat{K}_{tip} = K_B \Big/ \left(\sigma_{0i}\sqrt{c_0}\right),\ \hat{K}_{tip} = K_{tip} \Big/ \left(\sigma_{0i}\sqrt{c_0}\right)$$

K_L = Stress intensity factor due to applied remote loading

K_B = Stress intensity factor due to fiber bridging

K_{tip} = Crack tip toughness

σ_{0i} = Max. crack bridg. stress of aligned fiber with frict. bond

(expression is to be refered in Appendix)

$$c_0 = \left(\frac{L_f E_c}{2K_{tip}}\right)^2 \frac{\pi}{16\left(1-\nu^2\right)^2}$$

ν = Poisson's ratio of composite

$K_{tip} = K_m(E_c/E_m)$ can be assumed according to Marshall

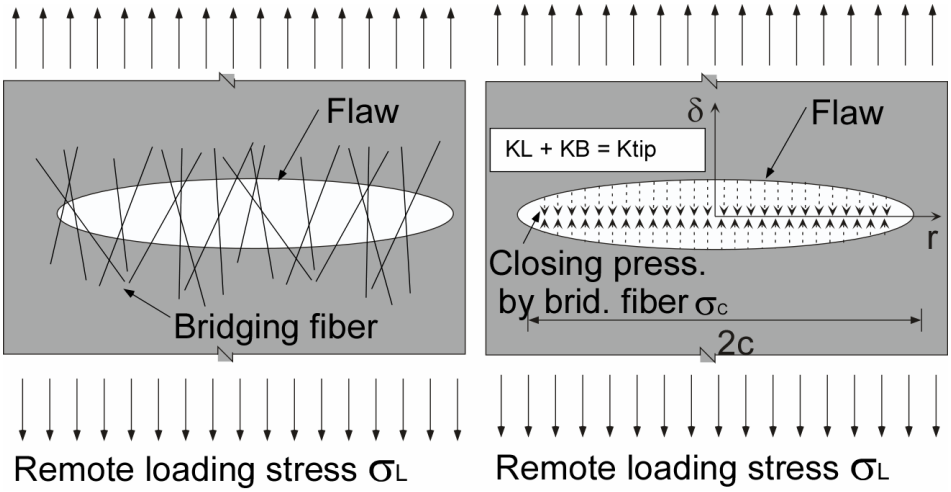

Fig. 2 Flaw model for cracking strength estimation.

et al. (1985), where K_m is matrix fracture toughness. K_L is expressed by hypothesizing a penny shaped crack in an infinite composite body subjected to remote loading σ,

$$K_L = 2\sqrt{\frac{\hat{c}}{\pi}}\hat{\sigma} \tag{6}$$

where,

$\hat{c} = c/c_0$, $\hat{\sigma} = \sigma/\sigma_{0i}$, and c = radius of crack

K_B may be obtained by integrating closure pressure due to fiber bridging over the crack profile as Li and Leung (1992):

$$\hat{K}_B = -2\sqrt{\frac{\hat{c}}{\pi}}\int_0^1 \hat{\sigma}_c(\hat{\delta})\frac{RdR}{\sqrt{1-R^2}} \tag{7}$$

where,

$$\hat{\delta} = \frac{\delta}{L_f/2}$$

$R = r/c$, *and* r=distance from crack center

Crack profile is not predetermined and σ_c is not known at a position with R in eq. (7). Following Li and Leung (1992), the crack profile is assumed for simplicity to take a half parabolic shape:

$$\hat{\delta} = \frac{1}{2}\sqrt{\hat{c}\left(1-R^2\right)} \tag{8}$$

For the fiber rupture type composites, eq. (7) is then calculated using the crack profile of eq. (8) and $\sigma_c(\delta)$ in eq. (3). For $\sigma_c(\delta)$, initial expression of $\sigma_{c1}(\delta)$ transits to $\sigma_{c2}(\delta)$ when fiber rupture initiates as shown in Appendix. Therefore, eq. (7) is modified accounting for fiber rupture as follows:

$$\hat{K}_B = -2\sqrt{\frac{\hat{c}}{\pi}}\left[\int_0^{R_u}\hat{\sigma}_{c2}(\hat{\delta})\frac{RdR}{\sqrt{1-R^2}} + \int_{R_u}^1 \hat{\sigma}_{c1}(\hat{\delta})\frac{RdR}{\sqrt{1-R^2}}\right] \tag{9}$$

where R_u denotes the crack radius within which fiber rupture occurs. R_u is expressed as follows:

$$R_u = \begin{cases} 0 & \text{for } \hat{\delta}_u(\phi=\pi/2) > \sqrt{\hat{c}}/2 \\ \sqrt{1-\dfrac{4\hat{\delta}_u(\phi=\pi/2)^2}{\hat{c}}} & \text{for } \hat{\delta}_u(\phi=\pi/2) \le \sqrt{\hat{c}}/2 \end{cases} \tag{10}$$

R_u is derived $\hat{\delta} = \hat{\delta}_u(\phi = \pi/2)$ is assumed in eq. (8). $\hat{\delta}_u(\phi = \pi/2)$ corresponds to COD at fiber rupture initiates and its expression is shown in Appendix.

Next, cracking stress level σ_{fc} is estimated by substituting eqs. (6) and (9) into eq. (5) and then solving for σ. Finally, σ_{fc} is obtained as a function of crack size c and micromechanical parameters of the composite:

$$\hat{\sigma}_{fc} = \frac{\sqrt{\pi}}{2\bar{c}}\left(\frac{\hat{K}_{tip}}{\hat{\delta}_{peak}}\right) + \left[\int_0^{R_u}\hat{\sigma}_{c2}(\hat{\delta})\frac{RdR}{\sqrt{1-R^2}} + \int_{R_u}^1 \hat{\sigma}_{c1}(\hat{\delta})\frac{RdR}{\sqrt{1-R^2}}\right] \tag{11}$$

where,

$\bar{c} = \sqrt{\hat{c}}/\hat{\delta}_{peak}$

$\hat{\delta}_{peak}$ = Normal. δ at peak bridg. stress $\hat{\sigma}_{\text{peak}}$ is attained

Note that σ_{fc} in eq. (11) is numerically calculated due to the mathematical complexity in the $\sigma_c(\delta)$ expression of eq. (3), unlike that for fiber pull-out type composites by Li and Leung (1992).

Equation (11) provides first cracking strength $(\sigma_{fc})_i$, when the flaw size "c" responsible for cracking is specified in the tensile specimens. This specification can be achieved experimentally such as by direct observation of flaw size in the composite. However, such flaw size investigation is beyond the scope of the current study. In this study, the flaw size c_m apparently responsible for matrix cracking is taken to be the same as that governing the composite's cracking, as a rough approximation. c_m is estimated assuming a penny-shaped flaw in an infinite composite bulk same as in deriving K_L in eq. (6).

$$c_m = \left(\frac{\sqrt{\pi}}{2}\frac{K_m}{\sigma_{mu}}\right)^2 \tag{12}$$

where,

K_m = Matrix fracture toughness

σ_{mu} = Tensile strength of plain matrix

Combining eqs. (11) and (12) leads to obtaining first cracking strength prediction, $\left(\sigma_{fc}\right)_i^{est}$, and two sources cause inaccuracy of estimating $\left(\sigma_{fc}\right)_i^{est}$. The first is additional flaws as air voids involved with fiber dispersion in mixing. Fiber involvement in mixing is likely to introduce additional defects in processing (Li and Mishra 1992). c_m in eq. (12) is estimated from matrix tensile strength, in which the above additional flaws due to processing are not taken into account. This discrepancy may be attributed to overestimating first cracking strength. The second source is due to the assumed elliptical crack shape in eq. (8). This simple assumption overestimates the crack opening and the closing pressure due to fiber bridging. Marshall *et al* (1985) conducted numerical simulation which suggested that the overestimation in cracking strength was up to 20%. Therefore,

considering the above two sources, this study suggests the following formula for estimating $\left(\sigma_{fc}\right)_i^{est}$ by introducing a reduction factor of 0.8.

$$\left(\hat{\sigma}_{fc}\right)_i^{est}=0.8\left\{\begin{array}{l}\dfrac{\sqrt{\pi}}{2\bar{c}_m}\left(\dfrac{\hat{K}_{tip}}{\hat{\delta}_{peak}}\right)\\ +\left[\int_0^{R_u}\hat{\sigma}_{c2}\left(\hat{\delta}\right)\dfrac{RdR}{\sqrt{1-R^2}}+\int_{R_u}^{1}\hat{\sigma}_{c1}\left(\hat{\delta}\right)\dfrac{RdR}{\sqrt{1-R^2}}\right]\end{array}\right\} \quad (13)$$

where,

$$\bar{c}_m=\sqrt{\hat{c}_m}\,/\,\hat{\delta}_{peak}$$

Finally, the procedure for estimating stress performance index $\sigma_{peak}/(\sigma_{fc})_i$, now read as $\sigma_{peak}/\left(\sigma_{fc}\right)_i^{est}$, is completed. This theoretical index is compared with the stress performance index observed in tests.

4. Experimental program

Focusing on the degree of multiple cracking saturation in fiber rupture type ECC, various ECC material mix designs resulting in different degrees of microcrack saturation will be demonstrated experimentally. This demonstration can be achieved by employing two approaches in ECC design, which increase the two performance indices described in the pervious section. One is to increase water-to-cement ratio (w/c, hereafter) in the matrix, and the other is to select fibers without chemical bonding with cementitious matrix.

These material constituent selections are justified by previous research results. Past studies have indicated that PVA fibers are characterized by high fiber strength and strong bonding with cementitious matrix (in comparison to those of polypropylene fibers, for example). However, it has been suggested that PVA fibers tend to have too strong interfacial friction bond strength τ_i and chemical bond strength τ_s. This intense interfacial bonding characteristic is reported to result in inadequate tensile strain capacity in PVA fiber composites (Kanda and Li 1999). Although strong bonding is generally preferable in fiber pull-out composites to achieve higher tensile strength and strain capacity, it is not necessarily the case for the fiber rupture type composites. Indeed, it has been quantitatively revealed that overly strong bond seriously reduces tensile strain capacity of the PVA fiber composites due to severe fiber rupture during crack bridging action and resulting in lower J'_b and J'_b/J_{tip} (Kanda and Li 1999). Weakening interfacial bond of PVA fibers can be achieved by employing matrix with higher w/c. This is supported by the evaluation results of single fiber pull-out bond tests, in which 14μm-PVA fiber's τ_i tend to decrease with increasing w/c of matrix (Kanda 1998). In addition to this bond weakening effects, increasing w/c of matrix is anticipated to enhance strain capacity by increasing J'_b/J_{tip} due to lower J_{tip}.

The second approach, selecting fibers without chemical bonding, is also reported to enhance J'_b/J_{tip} by increasing J'_b. Chemical bonding was theoretically revealed to increase the stiffness of crack bridging due to fiber. This higher stiffness leads to lower complementary energy J'_b and lower J'_b/J_{tip} (Kanda 1998). Chemical bonding is usually accompanied by hydrophilic fiber surface chemistry. Therefore, eliminating chemical bonding for PVA fibers may be achieved by changing their chemistry from hydrophilic to hydrophobic by fiber surface modification. This was recently achieved by Li and co-workers (2002). However, the current study selects a hydrophobic fiber for simplicity, a recently developed Polyethylene fiber with much smaller diameter (14 μm) than that of the 40μm-Polyethylene fiber used for the fiber pull-out type composites. The 14μm-Polyethylene fiber also has similar fiber strength and modulus as the 14μm-PVA fiber.

Thus, the current study investigates five different composites. **Table 1** summarizes these composites. This study employs the combination of two matrix mix proportions (w/c = 27 and 42 %) and three fiber types (14μm-PVA fiber, 40μm-PVA fiber, and 14μm-Polyethylene fiber). These composites are investigated by tensile test shown in **Fig. 3**. Of these combinations, two composites had been tested by the authors in the past (Kanda and Li 1999), and the remaining three were tested in the current study. The first two composites can be treated as the reference composites with low w/c and PVA fibers (14μm-PVA fiber composite with w/c = 27 % and 40μm-PVA fiber composite with w/c = 27 %). These composites have shown limited PSH behavior as indicated in **Fig. 4**. The three new composites tested are aimed at improving the multiple cracking saturation degree based on the observations of the reference composites and the two prescribed approaches. By increasing w/c of the reference systems, 14μm-PVA fiber composite with w/c = 42% and 40μm-PVA fiber composite with w/c = 42% were designed. Furthermore, instead of PVA fibers, 14μm-Polyethylene fiber was employed with w/c = 27% (14μm-Polyethylene fiber composite with w/c = 27%). This Polyethylene fiber has similar mechanical properties and geometry to the 14μm -PVA fiber. Matrix mix proportions for these composites are shown in **Table 2**.

Table 1 Outline of investigated composite.

W/C (1)	40 m-PVA (2)	14 m-PVA (3)	14 m-PE (4)
27%	○	○	◎
42%	◎	◎	-

◎: Tested ○: Referred to Kanda and Li 1999

It should be noted that all five composites in this study are designed to involve fiber rupture. This is confirmed in theory by adopting constitutive micromechanics parameters shown in **Table 3**. In this table some parameters are determined from past studies (e.g., Hirsch 1962; Ogishi and Ono 1987). Applying these parameters, the condition that ensures fiber rupture in composites is expressed as follows:

$$L_r < L_f \tag{14}$$

$L_r/2$ denotes minimum fiber embedment length where fiber rupture occurs in composites. A detailed expression of L_r should be referred to Appendix. All five composites satisfy the condition represented by eq. (14).

5. Experimental results and theoretical interpretation

Stress-strain curves were obtained in the uniaxial tensile tests as shown in **Fig. 5** and **Fig. 6**. Characterizing values representing stress-stain results in **Fig. 4**, **Fig. 5** and **Fig. 6** are summarized in **Table 4**. In this table, first cracking strength in test $\left(\sigma_{fc}\right)_i^{test}$ was determined as the first inflection point in stress-strain results as shown in **Fig. 7**. σ_{peak}^{test} denotes peak stress in stress-strain relation in tests. Furthermore, the ultimate tensile strain capacity ε_{cu}^{test} is defined as the strain beyond which continuous stress drop initiates.

Figure5 illustrates the stress-strain relation of the PVA composites with w/c = 42 %. Comparison of **Fig. 4** with **Fig. 5** reveals that higher w/c enhances the ultimate strain capacity ε_{cu}^{test}. From these two figures and **Table 4**, it is found that ε_{cu}^{test} extends from 0.26 % to 0.55 % on average with increasing w/c from 27% to 42% for the 14μm-PVA fiber composites. Furthermore, for the 40μm-PVA fiber composites, ε_{cu}^{test} increases from 1 % to 1.5 % on average as shown in **Table 4**. Therefore, it can be concluded that increasing w/c for PVA fiber composites is effective in enhancing PSH behavior as originally planned.

Figure 6 depicts the stress-strain relation of the Polyethylene fiber composite. In this figure, the strain capacity is much larger than that of the PVA fiber composites shown in **Fig. 4** and **Fig. 5**, reaching over 5 %. Hence the effect of using fiber with appropriate bond strengths was found to greatly enhance PSH behavior.

The observed effects of enhanced PSH can be examined from theoretical view points. Greater saturation of PSH behavior is led by higher potential in composite performance, which can be represented by the two performance indices, $\sigma_{peak}/(\sigma_{fc})_i$ and J'_b/J_{tip}, as described earlier. Indeed, the two adopted approaches to enhancing PSH behavior, increasing w/c for PVA fiber composites and using fiber with moderate bond strengths, were

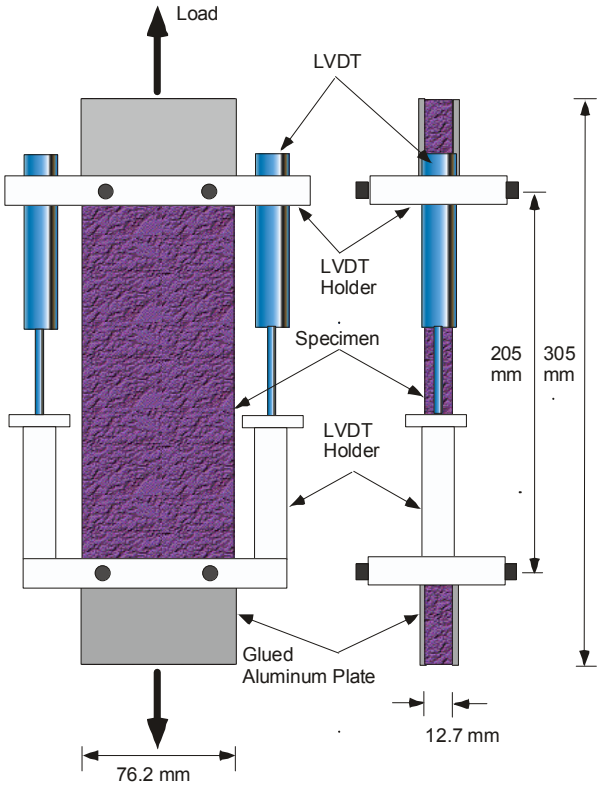

Fig. 3 Tensile test set-up.

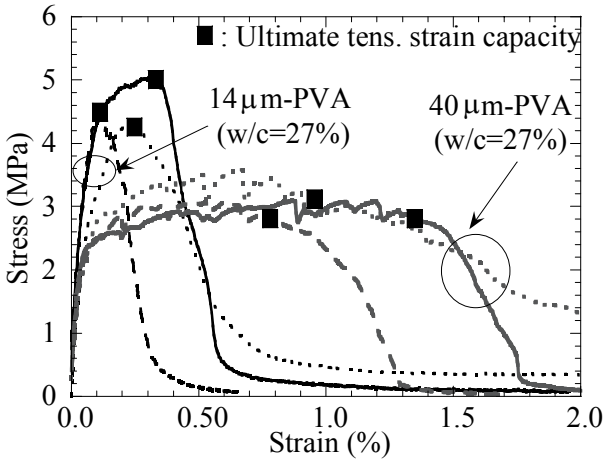

Fig. 4 Tensile stress-strain relation in test for 14μm-PVA and 40μm-PVA fiber composites with w/c =27%.

Table 2 Mix proportion of matrix.

W/C % (1)	Cement (2)	Silica fume (3)	Wtaer (4)	Super Plast. (5)	Viscous agent (6)
*27	0.8	0.2	0.27	0.040	-
42	1.0	-	0.42	0.007	0.0015

*Silica fume is included in cement weight

Table 3 Micromechanics parameter of composite.

Constituent	Micromechanics parameter	40μm-PVA		14μm-PVA		14μm-PE
		[a] w/c= 27%	w/c= 42%	[a] w/c= 27%	w/c= 42%	w/c= 27%
(1)	(2)	(3)	(4)	(5)	(6)	(7)
	Fiber length L_f (mm)	12		6		6
Fiber	Fiber diameter d_f (mm)	0.040		0.014		0.014
	Fiber elastic modulus E_f (GPa)	21.8		60		63
	Nominal fiber strength σ_{fu}^n (MPa)	806		1666		[e]1400
	Fiber volume fraction V_f (%)	2		1.5		2
Matrix	Matrix elastic modulus E_m (GPa)	23	[b]15.9	23	[b]15.9	23
	Matrix Fracture toughness K_m (MPa $m^{0.5}$)	0.33	[c]0.23	0.33	[c]0.23	0.33
	[g]Tensile strength σ_{mu} (MPa)	1.60	1.12	1.60	1.12	1.60
Fiber/ matrix interface	Frictional bond strength τ_l (MPa)	2.21	[d]2.21	4.35	[d]4.25	[f]0.66
	Chemical bond strength τ_s (MPa)	31.3	[d]31.3	33.6	[d]29.1	-
	Snubbing coefficient f	0.5	0.5	0.5	0.5	0.5
	Fiber strength reduction factor f'	0.3	0.3	0.3	0.3	0.3

[a] After Kanda and Li 1999 [b] After Hirsh 1962 [c] After Ogishi 1997 [d] After Kanda and Li 1998
[e] Assumed [f] After Li et.al 1995 [g] after Li et.al 1995

shown to increase these two indices as follows. They both decrease cracking stress level σ_{fc}, thus resulting in higher $\sigma_{peak}/(\sigma_{fc})_i$. This is demonstrated in **Fig. 8**, in which cracking stress level estimated via the proposed theory is depicted in terms of normalized crack size. Cracking stress curves in **Fig. 8** were obtained from eq. (11), whose micromechanical parameters were substituted using the magnitudes in **Table 3**. In **Fig. 8 (a)**, cracking stresses for the same crack size are found to decrease with increasing w/c in the PVA composites. Furthermore, the polyethylene fiber composite has much lower cracking stress than the PVA composites as shown in **Fig. 8 (b)**. Hence these differences in cracking stress appear to reflect variation in PSH saturation observed in the three composites.

Figure 9 further justifies the adopted approaches. This figure compares the crack bridging performances of the composites, which were estimated from eq. (3). It illustrates much higher complementary energy J'_b for the polyethylene fiber composite than the 14μm-PVA fiber composites. This appears to result in much greater saturation of PSH behavior in the former composite than in the latter. It should be noted that the 14μm-PVA fiber composite with w/c = 42 % has almost identical crack bridging performance and complementary energy J'_b to those with w/c = 27 %. However, the composite with w/c = 42 % appears to have lower crack tip toughness J_{tip} than

Table 4 Outline of tensile test result.

	40μm-PVA Comp.		14μm-PVA Comp.		14μm-PE Comp.
	w/c= 27% (1)	w/c= 42% (2)	w/c= 27% (3)	w/c= 42% (4)	w/c= 27% (5)
$\left(\sigma_{fc}\right)_i^{test}$	2.47	1.85	3.99	2.92	2.25
σ_{peak}^{test}	3.25	2.43	4.62	3.32	3.25
ε_{cu}^{test}	1.03	1.50	0.26	0.55	5.10

Data are the average of three specimens

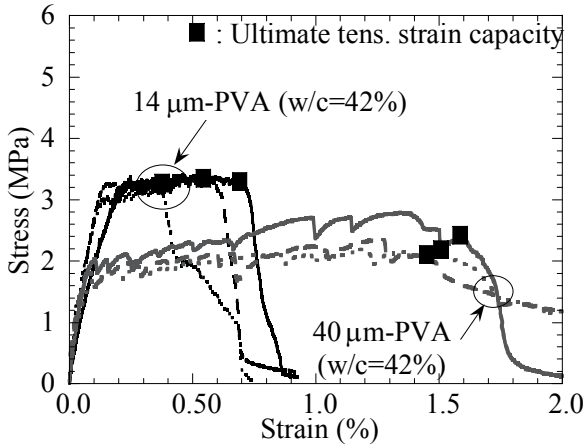

Fig. 5 Tensile stress-strain relation in test for 14μm-PVA and 40μm-PVA fiber composites with w/c =42%.

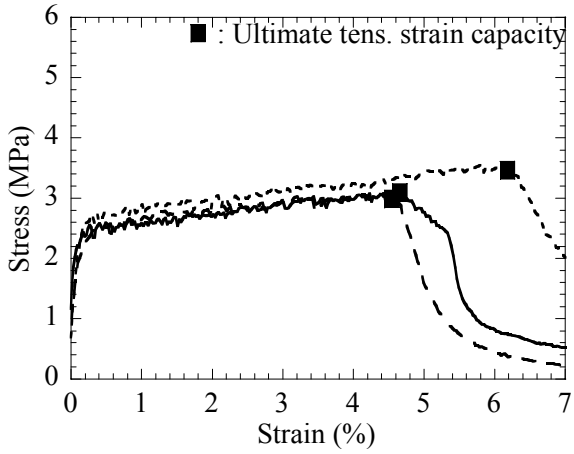

Fig. 6 Tensile stress-strain relation in test for14μm PE.

the one with w/c = 27 %. Literature suggests that this difference in J_{tip} is about 30 % (Ogishi and Ono 1987), which is likely to result in higher J'_b/J_{tip} and greater PSH saturation for the composite with w/c = 42 % than that

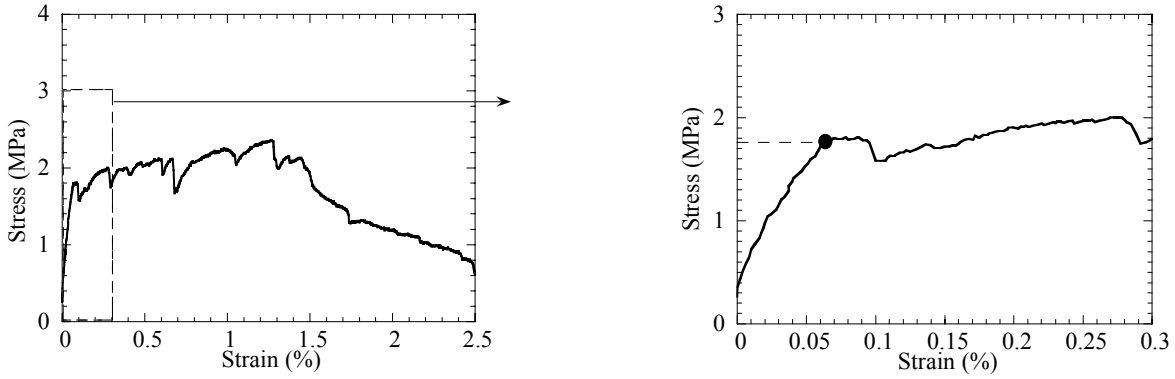

Fig. 7 Identification of first cracking point using stress-strain curve (40μm-PVA, w/c=42%).

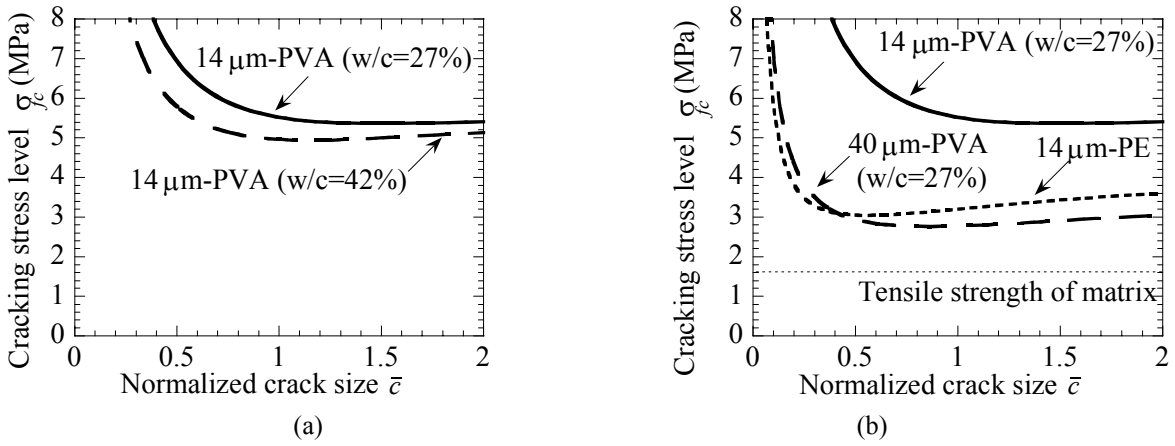

Fig. 8 Effect of experimental parameters on cracking stress level, (a) mix proportion, and (b) fiber type.

with w/c = 27 %.

Note that the polyethylene fiber composite should show much better PSH performance than the 14μm-PVA fiber composites even if these two composites involve the same fiber volume fraction of 1.5%. Although the examined polyethylene fiber composite contained 2% volume fiber, theoretical estimation showed that the polyethylene fiber composite with V_f = 1.5% still had higher potential for PSH performance than the examined 14μm-PVA fiber composite. The calculation revealed that the former composite had twice the J'_b/J_{tip} higher than the latter. The crack bridging performance of the former composite is shown as 14μm-PE (ref.) in **Fig. 9**.

6. Rationalizing theory for predicting performance indices

Prediction of two performance indices, J'_b/J_{tip} and $\sigma_{peak}/(\sigma_{fc})_i$ has to be rationalized with experimental results. J'_b/J_{tip} is not directly measured from tensile tests in this study. However, past study has demonstrated that this index predicted from the proposed theory shows strong correlation with ultimate tensile strain obtained from tensile tests using fiber rupture type composites (Kanda and Li 1999). Therefore, prediction procedure for J'_b/J_{tip} is considered to be justified in an indirect manner. $\sigma_{peak}/(\sigma_{fc})_i$ prediction for fiber rupture type composites is investigated first in this study and no previous comparison exists between test data and analysis prediction. This comparison is discussed below.

To analytically evaluate the stress performance index $\sigma_{peak}/(\sigma_{fc})_i$, accurate estimates of both peak bridging stress σ_{peak} and first cracking strength $(\sigma_{fc})_i$ are needed. Estimation of σ_{peak} is first validated by comparing test data and theoretical prediction. σ_{peak} is evaluated as the peak value of composite crack bridging performance: σ_c-δ relation of eq. (3). The evaluation results are plotted against test results in **Fig. 10**. In this figure, theoretical prediction σ_{peak} is rather consistent with σ_{peak}^{test} while only a data point in parenthesis, which corresponds to the 14μm-PVA fiber composite with w/c = 42 %, has over 50% estimation error. This error may be partially attributed to the so called "plug pull-out" phenomenon in crack bridging action of fiber (Li and Wu 1992; Naaman *et al*. 1991). This event is illustrated in **Fig. 11** and is not taken into account in the adopted theory.

In this plug pull-out phenomenon, adjacent fibers

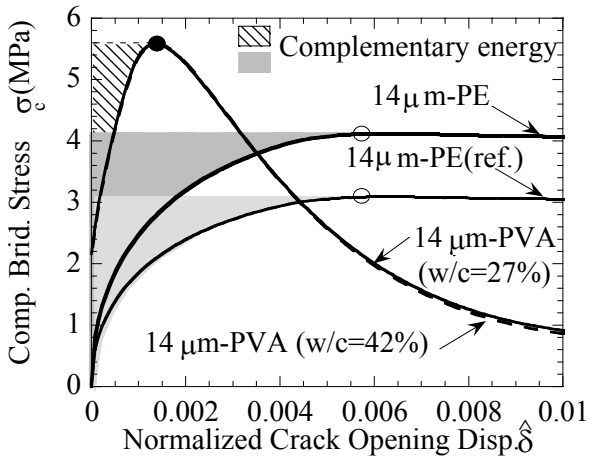

Fig. 9 Calculation result comparison in composite bridging performance.

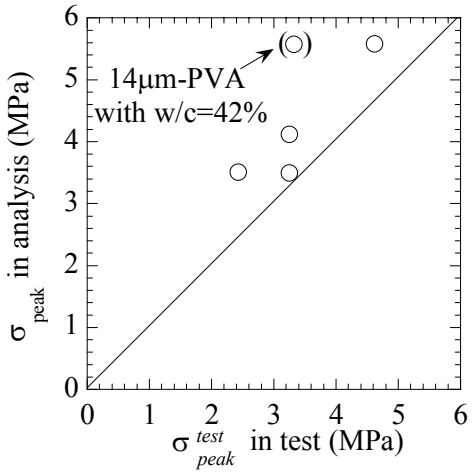

Fig. 10 Peak bridging stress comparison between test and analysis.

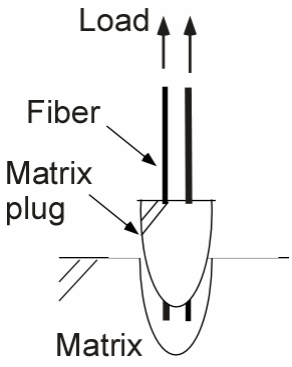

Fig. 11 Schematic of plug pull out phenomenon.

bridging across cracks are not pulled out individually but together with a small matrix block. This event occurs when matrix shear strength is rather weak relative to interfacial shear stress at fiber/matrix interface and limits fiber bridging performance to lower than expected. This appears to be the case for PVA fiber when high w/c is used. As described before, PVA fiber has very strong interfacial bond strengths with cement matrix. However, it is considered that the matrix with w/c = 42% has much lower shear strength than that with w/c = 27%. Some evidence of this plug pull-out event was described in the literature for the 14μm-PVA fiber composite with w/c = 42% (Kanda and Li 2002) in a microscope observation of crack plane, in which a few adjacent protruding fibers were together with a matrix plug. However, other composites including the 40μm-PVA fiber composite with w/c = 42% did not show significant plug pull-out events. This may be because that frictional bond strength of 40μm-PVA fiber is about half that of 14μm-PVA and distance between fibers is considered much larger than the other due to its much larger fiber diameter and length. In the following investigation, data for 14μm-PVA fiber composite with w/c = 42% are excluded due to this plug pull-out phenomenon.

The proposed theory for determining first cracking strength is justified in this study using uniaxial tensile test data. First, cracking strength observed in tensile tests, $\left(\sigma_{fc}\right)_i^{test}$, was determined as the first inflected point in the obtained stress-strain curves as depicted in **Fig. 7**. Furthermore, theoretical first cracking strength, $\left(\sigma_{fc}\right)_i^{est}$, was estimated from eq. (13). The comparison between $\left(\sigma_{fc}\right)_i^{est}$ and $\left(\sigma_{fc}\right)_i^{test}$ is illustrated in **Fig. 12**, where the estimation results of $\sigma_{fc}(c_m)$ using eqs. (11) and (12) without reduction factor of 0.8 is also involved as a reference. Calculating c_m requires the estimation of σ_{mu} for each composite, which is achieved by referring literature (Li *et al*. 1995). In **Fig. 12**, $\left(\sigma_{fc}\right)_i^{est}$ appears much more coincident with $\left(\sigma_{fc}\right)_i^{test}$ than $\sigma_{fc}(c_m)$, which overestimates by 45 % on average for the current data set. Therefore, introducing the reduction factor in eq. (13) appears valid and this suggested formula seems to reproduce test results of first cracking strength.

Next, accuracy in estimating stress performance index $\sigma_{peak}\Big/\left(\sigma_{fc}\right)_i^{est}$ is demonstrated by comparison with test data as shown in **Fig. 13**. This figure shows reasonable agreement between stress performance indices obtained from test and analysis. This result substantiates the proposed theory in estimating stress performance index. Hence it can be concluded that theoretical stress performance index using the proposed first cracking strength formula is coincident with the actual performance index.

Note that the c_m obtained from eq. (12) was too large compared with realistic flaw size observation in composite (Kanda and Li 2000). This discrepancy appears to be attributed to the hypothesis adopted in eq. (12), in

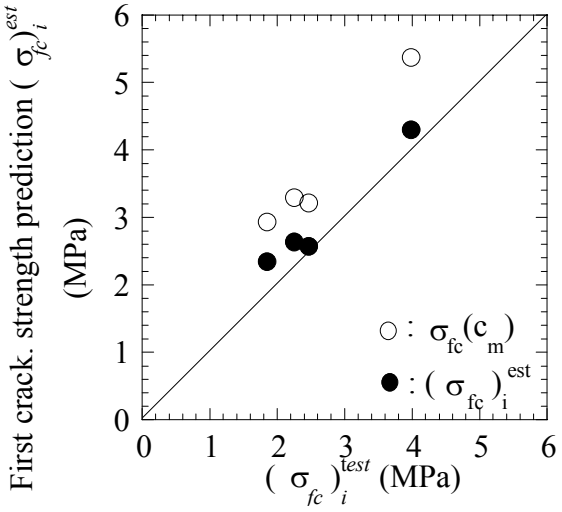

Fig. 12 First cracking strength comparison between test and analysis.

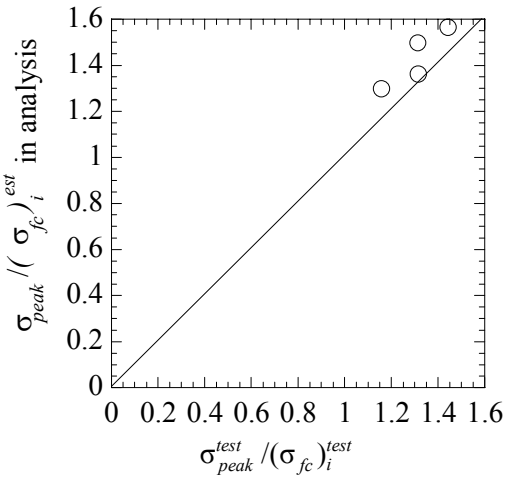

Fig. 13 Stress performance index comparison between test and analysis.

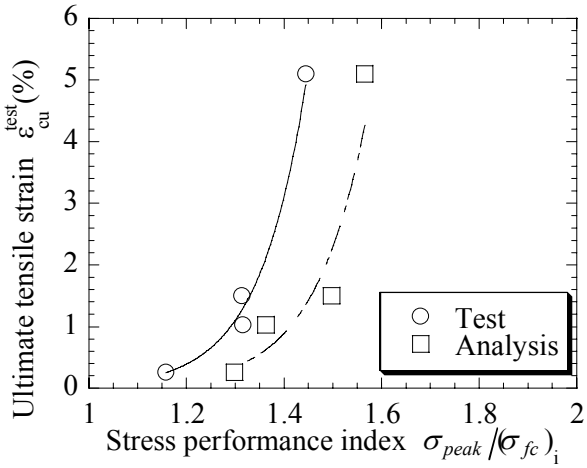

Fig. 14 Effect of stress performance index on ultimate tensile strain.

which a penny shaped single crack is assumed for simplicity to occur in infinite bulk solid of materials. In reality, however, numerous cracks are present; their interaction increases the Stress Intensity Factor (SIF). Accounting for this interaction effect in the formula leads to smaller and more realistic estimation of flaw size. Nevertheless, first cracking strength formula in eq. (13) was derived under the same hypothesis as eq. (12). This means that using c_m evaluated by eq. (12) appears to lead to reasonable estimation of first cracking strength using eq. (13). Indeed, this is demonstrated in **Fig. 12**. However, a more advanced hypothesis (e.g., random flaws interacting with each other in composites) is needed to more accurately determine c_m and first cracking strength in analysis in a future study.

7. Effect of performance indices on ultimate tensile strain

The inclination of ultimate tensile strain is checked with the proposed performance indices, $\sigma_{peak}/\left(\sigma_{fc}\right)_i$ and J'_b/J_{tip}. **Figure 14** illustrates the relationship between $\sigma_{peak}/\left(\sigma_{fc}\right)_i^{est}$ and observed ultimate strain ε_{cu}^{test}. In **Fig. 14**, open circles indicate the stress performance index observed in the tests, $\sigma_{peak}^{test}/\left(\sigma_{fc}\right)_i^{test}$, and solid circles indicate theoretical values, $\sigma_{peak}/\left(\sigma_{fc}\right)_i^{est}$, estimated from eqs. (3) and (13). **Figure 14** shows that increasing $\sigma_{peak}/\left(\sigma_{fc}\right)_i^{est}$ leads to higher ε_{cu}^{test}. This tendency reflects that higher stress potential ensures better conformance for stress criterion of PSH behavior, given by eq. (1). The dependency of ε_{cu}^{test} on $\sigma_{peak}/\left(\sigma_{fc}\right)_i^{est}$ is very similar to that on $\sigma_{peak}^{test}/\left(\sigma_{fc}\right)_i^{test}$ as demonstrated in **Fig. 14** while the theoretical performance index is slightly (about 10%) larger than observed value for the identical ε_{cu}^{test}. For energy performance index J'_b/J_{tip}, **Figure 15** shows relationship with observed ultimate strain ε_{cu}^{test}. In this figure, ε_{cu}^{test} coincides with increasing J'_b/J_{tip}, which is similar to the case for $\sigma_{peak}/\left(\sigma_{fc}\right)_i^{est}$.

The results in **Fig. 14** and **Fig. 15** agree with those for fiber pull-out type ECC in a past study (Kanda and Li 1998) and infers the possibility of controlling the PSH saturation intensity via ultimate tensile strain in terms of the two performance indices. However, ultimate tensile strain is influenced by both crack opening displacement and crack spacing. The latter directly correlates with PSH saturation intensity, and this correlation is investigated next.

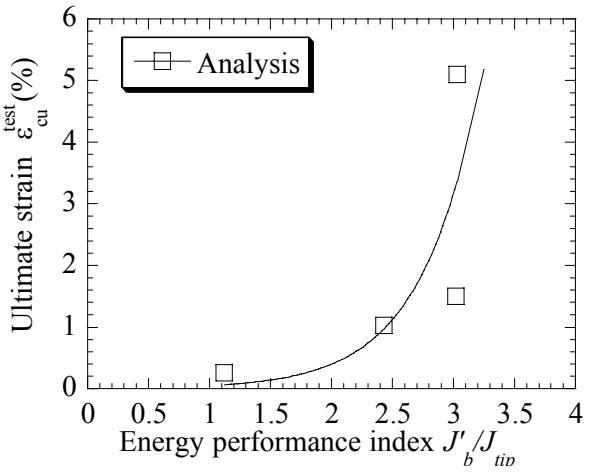

Fig. 15 Effect of energy performance index on ultimate tensile strain.

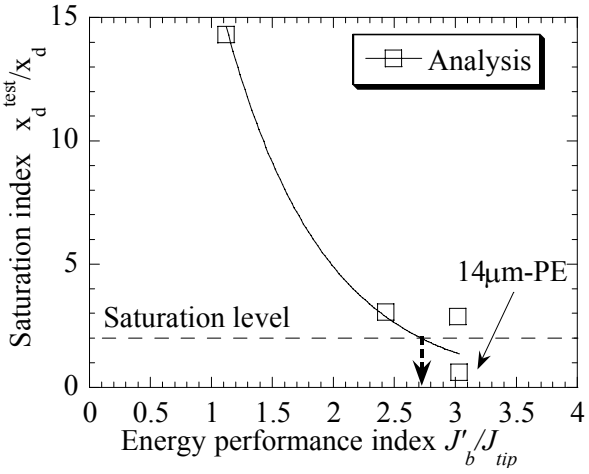

Fig. 16 Effect of energy performance index on saturation index.

8. Composite design criteria with performance indices

The two performance indices, $\sigma_{peak}/(\sigma_{fc})_i$ and J'_b/J_{tip}, are utilized to propose practical criteria for designing saturated fiber rupture type ECC with saturated PSH behavior. For this purpose, an index for measuring PSH saturation is introduced, and its limiting value to achieve saturated PSH is defined referring to past studies. Next, relationship between the saturation index and the performance indices is shown. Then design criteria in terms of the two performance indices, above which saturated PSH behavior is expected, are finally investigated using the relationship with the saturation index.

Saturation intensity of PSH behavior may be measured using the saturation index, expressed as the ratio between observed ultimate crack spacing in tests, x_d^{test}, and theoretical saturated crack spacing, x_d (Kanda and Li 1998b). x_d is defined as crack spacing necessary to transfer stress from bridging fibers to matrix via interface friction in a cracked section. Micromechanics theory for predicting x_d has been proposed in the literature (Wu and Li 1995):

$$x_d = \frac{L_f - \sqrt{L_f^2 - 2\pi\psi L_f x}}{2} \tag{15}$$

where,

$$\psi = \frac{4}{\pi g},\ x = \frac{(1-V_f)\sigma_{mu} d_f}{4V_f \tau_i},\ \text{and}\ g = \frac{2(1+e^{\pi f/2})}{4+f^2}$$

Note that this formula neglects the effect of chemical bond strength τ_s. Therefore, x_d obtained from eq. (15) is considered a higher bound in this study. Furthermore, x_d^{test} is assumed by employing ε_{cu}^{test} and δ_{peak}, which is crack opening displacement δ at peak stress attained in composite bridging performance σ_c—δ relation with eq. (3) (Lin and Li 1997):

$$x_d^{test} = \delta_{peak}/\varepsilon_{cu}^{test} \tag{16}$$

Saturation index x_d^{test}/x_d was then evaluated from the tensile test results and these two equations.

It is found that practical criteria for saturated PSH can be expressed in terms of the two performance indices. In **Fig. 16**, the saturation index x_d^{test}/x_d is plotted against the energy performance index J'_b/J_{tip}. The broken horizontal line in **Fig. 16**, $x_d^{test}/x_d = 2$ was proposed as a design limit, above which saturated PSH behavior is rarely expected (Kanda and Li 1998b). This broken line crosses x_d/x_d^{test} — J'_b/J_{tip} curve near $J'_b/J_{tip} = 2.7$, which is considered as design criterion for saturated PSH in terms of energy performance. $J'_b/J_{tip} > 3$ was also proposed as the design criterion for saturated PSH behavior for fiber pull-out type composites, which is similar to the above obtained results for the fiber rupture type (Kanda and Li 1998b). In **Fig. 17**, the saturation index x_d^{test}/x_d is plotted against the stress performance index $\sigma_{peak}/(\sigma_{fc})_i$, which suggests that $\sigma_{peak}/(\sigma_{fc})_i^{test} > 1.35$ is necessary to achieve saturated PSH. This condition is slightly larger than that reported for the fiber pull-out type composites (> 1.2) (Kanda and Li 1998b). In **Fig. 17**, the x_d^{test}/x_d — $\sigma_{peak}/(\sigma_{fc})_i^{est}$ curve is illustrated as well. This theoretical curve is close to the test observation, x_d^{test}/x_d — $\sigma_{peak}/(\sigma_{fc})_i^{test}$, while it slightly underestimates the test results. Therefore, $\sigma_{peak}/(\sigma_{fc})_i^{est} > 1.3$ may be employed as a practical stress criterion.

The above discussion with **Fig. 16** and **Fig. 17** suggests that fiber rupture type ECCs can be designed with

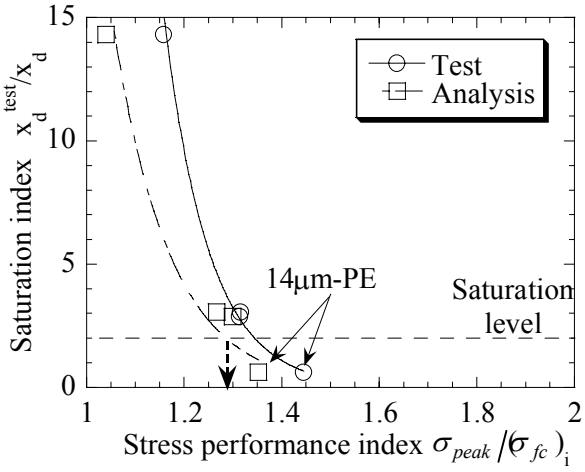

Fig. 17 Effect of stress performance index on saturation index.

saturated PSH by considering J'_b/J_{tip} > 2.7 and $\sigma_{peak}\Big/\left(\sigma_{fc}\right)_i^{est}$ > 1.3 as a reference. The major significance is that the design considerations with these criteria are essentially conducted by theory without experiments for composites similar to those involved in the present data set. However, the present data set covers rather a broad range of variation in micromechanical parameters, e.g., different fiber type, fiber length, fiber diameter, and matrix type. Hence these minimum performance indices may be used as comprehensive design references. Of course, more research results should be accumulated to practically employ these design criteria with confidence.

It should be noted that the above two criteria need to be simultaneously satisfied in achieving saturated PSH behavior. For example, ECCs designed to satisfy J'_b/J_{tip} > 2.7 may not show saturated PSH behavior when they involve flaws with very small size c_m. Smaller c_m increases first cracking strength as shown in eq. (13) and results in violating $\sigma_{peak}\Big/\left(\sigma_{fc}\right)_i^{est}$ > 1.3. In another example, a composite involving large flaw size may result in satisfying $\sigma_{peak}\Big/\left(\sigma_{fc}\right)_i^{est}$ > 1.3. However, unless J'_b/J_{tip} > 2.7 is satisfied, steady state cracking may not be ensured on each crack plane. This means this composite does not show PSH behavior.

9. Conclusions

This study has focused on design and demonstration of fiber rupture type ECCs with saturated Pseudo Strain Hardening behavior. As a result, saturated PSH behavior was experimentally observed for the fiber rupture type ECCs in uniaxial tensile tests by tailoring composite constituents. The process of designing these composites is facilitated by the newly proposed practical design criteria using micromechanics, which are based on two performance indices: stress performance index $\sigma_{peak}\Big/\left(\sigma_{fc}\right)_i$ and energy performance index J'_b/J_{tip}.

Evaluation of $\sigma_{peak}\Big/\left(\sigma_{fc}\right)_i$ necessitates the extension of the theory for estimating first cracking strength $(\sigma_{fc})_i$ in the literature. This precedent theory is limited in covering composite constituent properties, i.e., complete fiber pull-out without rupturing and friction dominant fiber/matrix interface with negligible chemical bonding. Accounting for fiber rupture and chemical bond, this study proposed a comprehensive theory for first cracking strength with correction factor of 0.8, which is necessary due to simplified crack profile and underestimated flaw size responsible to cracking. The comparison with test data revealed that prediction with the proposed theory matches measured first cracking strength within 10 % error.

The two performance indices were evaluated for four different composites tested in uniaxial tension. Correlations between PSH saturation intensity and these performance indices suggest the following practical design criteria for PSH in fiber rupture type ECCs, $\sigma_{peak}\Big/\left(\sigma_{fc}\right)_i^{est}$ > 1.3 and J'_b/J_{tip} > 2.7. These criteria were almost comparable to those obtained for fiber pull-out type ECC in the literature. Furthermore, the data set used for obtaining these criteria cover a rather broad range of micromechanical parameters. Therefore, these criteria may be applied for various types of composites e.g., independent of existing fiber rupture and chemical bond. In fact, both indices are fundamentally governed by matrix types and fiber bridging properties. The effects of fiber pull-out or rupture are reflected in these indices.

This study proposed design criteria for achieving PSH composites, which should be practical and comprehensive. Because this guideline appears to be supported by limited test data, further investigation is necessary to assure reliability.

Acknowledgements

This study was based on T. Kanda's Ph. D thesis submitted to the University of Michigan. T. Kanda appreciates useful discussion with Dr. Takashi Matsumoto at the University of Tokyo.

References

Hirsch, T. J. (1962). "Modulus of Elasticity of Concrete Affected by Elastic Moduli of Cement Paste Matrix and Aggregate." *Journal of the American Concrete Institute* (March), 427-449.

Kanda, T. and Li, V. C. (1998). "Interface Property and Apparent Strength of a High Strength Hydrophilic Fiber in Cement Matrix." *ASCE J. Materials in Civil Engineering*, 10 (1), 5-13.

Kanda, T. and Li, V. C. (1998). "Multiple Cracking Sequence and Saturation in Fiber Reinforced Cementitious Composites." *Concrete Research and Technology, Japan Concrete Institute*, 9 (2), 1-15.

Kanda, T. and Li, V. C. (1999). "Effect of Apparent Strength and Fiber-Matrix Interface Properties on Crack Bridging in Cementitious Composites." *Journal of Engineering Mechanics, ASCE*, 125 (3), 290-299.

Kanda, T. and Li, V. C. (1999). "New Micromechanics Design Theory for Pseudo Strain Hardening Cementitious Composite." *Journal of Engineering Mechanics*, *ASCE*, 125 (4), 373-381.

Kanda, T. and Li, V. C. (2000). "Modeling of Tensile Stress-Strain Relation of Pseudo Strain Hardening Cementitious Composites." *Journal of Materials in Civil Engineering*, 12 (2), 147-156.

Kanda, T. and Li, V. C. (2002). "Practical Design Guidelines for Pseudo Strain Hardening Cementitious Composites Reinforced with Short Random Fibers (in Japanese)." *J. Struct. Constr. Earthquake Eng*. (552), 13-21.

Leung, C. K. Y. (1996). "Design Criteria for Pseudoductile Fiber-Reinforced Composites." *Journal of Engineering Mechanics*, *ASCE*, 22 (1), 10-14.

Li, V. C. (1993). "From Micromechanics to Structural Engineering · The Design of Cementitious Composites for Civil Engineering Applications." *J. Struct. Mech. Earthquake Eng*., *JSCE*, 10 (2), 37-48.

Li, V. C. and Leung, K. Y. (1992). "Steady-state and Multiple Cracking of Short Random Fiber Composites." *Journal of Engineering Mechanics*, *ASCE,* 118 (11), 2246-2263.

Li, V. C. and Mishra, D. K. (1992). "Micromechanics of Fiber Effect on the Uniaxial Compressive Strength of Cementitious Composites." Fiber Reinforced Cement and Concrete, RILEM, R. N. Swamy, ed., 400-414.

Li, V. C., Mishra, D. K. and Wu, H. C. (1995). "Matrix Design for Pseudo-Strain Hardening Fiber Reinforced Cementitious Composites." *Materials and Structures, RILEM*, 28, 586-595.

Li, V. C., Wang, Y. and Backer, S. (1990). "Effect of Inclining Angle, Bundling, and Surface Treatment on Synthetic Fiber Pull-out from a Cement Matrix." *Composites*, 21 (2), 132-140.

Li, V. C., Wu, C., Wang, S., Ogawa, A. and Saito, T. (2002). "Interface Tailoring for Strain-hardening PVA-ECC." *ACI Materials Journal*, 99 (5), 463-472.

Marshall, D. B. and Cox, B. N. (1988). "A J-Integral Method for Calculating Steady-State Matrix Cracking Stresses in Composites." *Mechanics of Materials*, 7, 127-133.

Marshall, D. B., Cox, B. N. and Evans, A. G. (1985). "The Mechanics of Matrix Cracking in- Brittle-Matrix Fiber Composites." *Acta Metallurgica*, 33 (11), 2013-2021.

Naaman, A. E. and Reinhardt, H. W. (1995). "High Performance Fiber Reinforced Cement Composites 2 (HPFRCC2)." RILEM Proceedings 31, E&FN Spon, London.

Ogishi, S. and Ono, H. (1987). "Effects of Experimental Parameters on Fracture Toughness of Cement Paste and Mortar, Japan Concrete Institute." *Concrete Journal*, *JCI*, 25 (2), 113-125.

Appendix full expression of bridging law

For $\hat{L}_r < 2$ and $1 < \hat{L}_c$

$$\sigma_c = \begin{cases} \sigma_{0i}\, {}_dC_A G\left(\frac{\pi}{2}, f\right) & \text{for } 0 \le \frac{\delta}{\delta_u\left(\phi=\frac{\pi}{2}\right)} \le 1 \\ \sigma_{0i}\left\{ \begin{matrix} {}_dC_A G(\phi_c, f) + {}_dC_{B2} A(\phi_c, -f-2f') \\ + {}_dC_{B3} A(\phi_c, -f') + {}_dC_{B4} A(\phi_c, f) \end{matrix} \right\} & \text{for } 1 < \frac{\delta}{\delta_u\left(\phi=\frac{\pi}{2}\right)} \end{cases} \quad \text{(A-1)}$$

For $\hat{L}_c < 1$

$$\sigma_c = \begin{cases} \sigma_{0i}\, {}_dC_A G\left(\frac{\pi}{2}, f\right) & \text{for } 0 \le \frac{\delta}{\delta_u\left(\phi=\frac{\pi}{2}\right)} \le 1 \\ \sigma_{0i}\left\{ \begin{matrix} {}_dC_A G(\phi_c, f) + {}_dC_{B2} A(\phi_c, -f-2f') \\ + {}_dC_{B3} A(\phi_c, -f') + {}_dC_{B4} A(\phi_c, f) \end{matrix} \right\} & \text{for } 1 < \frac{\delta}{\delta_u\left(\phi=\frac{\pi}{2}\right)} \end{cases} \quad \text{(A-2)}$$

where,

$$\sigma_{0i} = \frac{V_f \tau_i}{2}\left(\frac{L_f}{d_f}\right)$$

$${}_dC_A = -\gamma + 2\gamma^{\frac{1}{2}} + \left(\frac{\sigma_{ds}}{\lambda}\right)^2, \quad {}_dC_{B2} = \left(\frac{\sigma_{fu}^n}{\lambda}\right)^2$$

$${}_dC_{B3} = -2\xi\left(\frac{\sigma_{fu}^n}{\lambda}\right)^2, \quad {}_dC_{B4} = \left[\xi\left(\frac{\sigma_{fu}^n}{\lambda}\right)\right]^2, \quad {}_dC_C = 1$$

$$\gamma = \left(\frac{E_f}{\lambda}\right)\bar{\delta} + \left(\frac{\sigma_{ds}}{\lambda}\right)^2, \quad \xi = \left(\frac{\sigma_{ds}}{\lambda}\right) \Big/ \left(\frac{\sigma_{fu}^n}{\lambda}\right)$$

$$\hat{\phi}_c(\hat{\delta}) = \begin{cases} \dfrac{\pi}{2} & \text{for } 0 \le \dfrac{\delta}{\delta_u\left(\phi=\dfrac{\pi}{2}\right)} \le 1 \\ -\dfrac{1}{2(f+f')} \ln\left[\left(\dfrac{Ef}{\lambda}\right)\bar{\delta} \Big/ \left(\dfrac{\sigma_{fu}^n}{\lambda}\right)^2 + \xi^2\right] & \\ & \text{for } 1 < \dfrac{\delta}{\delta_u\left(\phi=\dfrac{\pi}{2}\right)} \end{cases}$$

$$\delta_u\left(\phi=\frac{\pi}{2}\right) = \frac{\lambda}{Ef(1+\eta)}\left[e^{-(f+f')\pi} - \xi^2\right]$$

$$\hat{L}_c = \left(\frac{\sigma_{fu}^n}{\lambda}\right)(1-\xi),\ \hat{L}_r = 2\left(\frac{\sigma_{fu}^n}{\lambda}\right)\left[e^{-(f+f')\frac{\pi}{2}} - \xi\right]$$

$$G(\phi,\alpha) = \frac{1}{\alpha^2+4}\left\{e^{\alpha\phi}[\alpha\sin 2\phi - 2\cos 2\phi] + 2\right\}$$

$$A(\phi,\alpha) = \frac{1}{\alpha^2+4}\left\{e^{\alpha\phi}[2\cos 2\phi - \alpha\sin 2\phi] + 2e^{\frac{\pi}{2}\alpha}\right\}$$

$$B(\phi_1,\phi_2,\alpha) = \frac{1}{\alpha^2+4}\left\{\begin{matrix} e^{\alpha\phi_2}[\alpha\sin 2\phi_2 - 2\cos 2\phi_2] \\ + e^{\alpha\phi_1}[2\cos 2\phi_1 - \alpha\sin 2\phi_1] \end{matrix}\right\}$$

Notation

d_f = fiber diameter;
E_c = elastic modulus of composite;
E_f = elastic modulus of fiber;
E_m = elastic modulus of matrix;
K_B = stress intensity factor due to fiber bridging;
K_L = stress intensity factor by applied remote loading;
K_m = matrix fracture toughness;
K_{tip} = crack tip toughness;
f = snubbing coefficient;
f' = fiber strength reduction factor;
J_{tip} = crack tip toughness (energy form)
J'_b = complementary energy of σ_c-δ curve;
L_c = maximum critical fiber embedment length;
L_r = minimum fiber length for fiber rupture;
L_f = fiber length;
V_f = volume fraction of fiber;
δ = crack opening displacement;
ε_{cu}^{test} = Ultimate tensile strain capacity in test;
σ_c = crack bridging stress of composite;
σ_{peak} = peak bridging stress of composite;
$\left(\sigma_{fc}\right)_i^{est}$ = irst cracking strength in theory;
$\left(\sigma_{fc}\right)_i^{test}$ = first cracking strength in test;
σ_{peak}^{test} = peak composite bridging stress in test;
x_d = saturated crack spacing;
x_d^{test} = crack spacing in test;
τ_I = frictional bond strength;
τ_s = chemical bond strength;

superscripts

(^) = normalization by $L_f/2$;